J Plant Growth Regul (2008) 27:26–38
DOI 10.1007/s00344-007-9027-2

The Auxin Conjugate Hydrolase Family of *Medicago truncatula* and Their Expression During the Interaction with Two Symbionts

James J. Campanella · Stephanie M. Smith · Dora Leibu · Shiri Wexler · Jutta Ludwig-Müller

Received: 26 January 2007 / Accepted: 5 July 2007 / Published online: 25 September 2007

Abstract We have characterized the regulation of auxin conjugate hydrolysis in *Medicago truncatula* during development and interaction with two symbionts. In *Medicago truncatula* five putative auxin amidohydrolase genes (*MtIAR31*, *MtIAR32*, *MtIAR33*, *MtIAR34*, *MtIAR36*) were identified, homologous to the *AtIAR3* gene from *Arabidopsis thaliana*. The *MtIAR32* transcript is the most abundant transcript in whole seedlings after germination, whereas *MtIAR33* is the least abundant. *MtIAR32* is also the most abundant transcript in adult roots, stems, and basal leaves. *MtIAR31* is most highly expressed in flowers and *MtIAR36* in terminal leaves. *Sinorhizobium meliloti*-infected seedlings primarily upregulated *MtIAR33* and *–34* transcripts. *Glomus intraradices*-infected seedlings upregulated *MtIAR33* and *–34*. MtIAR31, –32, –33, and –34 have hydrolytic activity against IAA-aspartate and IBA-alanine. MtIAR33, –34, and –36 hydrolyze the ester bonds of IAA-glucose. MtIAR36 solely possesses activity against IAA-glycine, -alanine, and -isoleucine. IBA was increased in *Glomus intraradices*-inoculated roots of *Medicago* compared to controls, whereas IAA was not. Our results suggest an intricate control system that regulates free and conjugated auxins in *Medicago*.

J. J. Campanella (✉) · S. M. Smith · D. Leibu · S. Wexler
Department of Biology and Molecular Biology,
Montclair State University, 1 Normal Avenue, Montclair,
New Jersey 07043, USA
e-mail: james.campanella@montclair.edu

J. Ludwig-Müller
Institut für Botanik, Technische Universität Dresden,
Zellescher Weg 20b, 01062 Dresden, Germany

Keywords *Medicago truncatula* · Auxin amidohydrolases · Auxin · Symbiosis · Arbuscular mycorrhiza · Nodulation

Introduction

Regulation of host-symbiont interaction is of great interest to those who study both plant and symbiote physiology. Our studies have focused specifically on two such processes in the model legume *Medicago truncatula*: fungal colonization, leading to arbuscular mycorrhiza (AM) formation, and bacterial invasion, leading to root nodulation. Plant hormones can be considered important signals in establishing relationships between plants and microbes. The exchange of signals during the initial phases of symbiosis is crucial for the regulation of an intricate relationship between organisms. Phytohormones may constitute at least part of these signals (Barker and Tagu 2000; Ludwig-Müller 2000).

The hypothetical involvement of auxins in nodule development is feasible because they are highly organized structures, similar to lateral roots (Hirsch and La Rue 1997). Mathesius and others (1998) provided evidence that levels of auxins were increased in cells that divide to form the root nodule primordium. More recently, root nodule studies have demonstrated that ethylene, auxin, and cytokinin are involved in controlling or mediating symbiotic responses (Mulder and others 2005).

Several lines of evidence suggest a role for auxin at different stages in nodule organogenesis (de Billy and others 2001; Roudier and others 2003). First, synthetic auxin transport inhibitors can induce the development of pseudonodules on plant roots (Hirsch and others 1989). Second, auxin localization is correlated with the site of

cortical cell division. Auxin was localized in *Lotus japonicus* and white clover roots during nodulation (Mathesius and others 1998; Pacios-Bras and others 2003). Third, de Billy and others (2001) demonstrated that import carrier genes in *Medicago* are expressed predominantly in regions of root tips and nodule primordia, suggesting that auxin is required for primordia and vasculature development. Further genetic evidence from Wasson and others (2006) supports the hypothesis that auxin transport is involved in nodulation in *Medicago* and that root flavonoids act as regulators. Inoculation with rhizobia reduced auxin transport in control roots after 24 h, similar to the action of the auxin transport inhibitor *N*-(1-naphthyl)phthalamic acid (NPA) (Wasson and others 2006). Rhizobia were unable to reduce auxin transport in flavonoid-deficient roots, even though NPA inhibited auxin transport. This result was confirmed by Huo and others (2006), directly showing a role for polar auxin transport in nodule development in *Medicago* using RNAi plants for the *Medicago* PIN1 auxin carrier.

The role of auxin during arbuscular mycorrhiza (AM) formation is less well understood. In maize, Ludwig-Müller and others (1997) observed an increase of the auxin indole-3-butyric acid (IBA) in inoculated roots concomitant with the enzyme activity for IBA synthesis. In addition, exogenous IBA altered maize root morphology in the same way as AM formation (Kaldorf and Ludwig-Müller 2000). Auxin conjugates also increased during AM colonization in maize roots at later time points (Fitze and others 2005).

Elevated auxin levels have also been reported for soybean (Meixner and others 2005) and nasturtium (Jentschel and others 2007) during AM colonization, so it can be concluded that the increase in auxin levels is observed in the AM symbiosis in at least three plant species. Based on these data, we have hypothesized that changes in auxin concentrations may play a role in the regulation of AM formation in *Medicago* and, by extension, the symbiotic process of nodulation.

In this work we have investigated the possibility that auxin conjugate hydrolysis could contribute to elevated free auxin levels in the rhizobium and to AM interaction in the model legume *Medicago truncatula*. To better examine this hypothesis, our goal was to isolate and characterize the genes involved in the regulation of auxin homeostasis in the model legume *Medicago* and to examine any induced changes in the transcription of these genes during the initial interactions between host and symbiote.

Free auxin levels are regulated in higher plants by, among other factors, auxin conjugate hydrolases. Auxin, primarily indole-3-acetic acid (IAA) and IBA, is stored in conjugated forms that are generally considered to be inactive. Two major types of conjugates have been examined: (1) those bound to one or more amino acids and (2) those ester-linked forms bound to sugar(s). Both types may be found at varying concentrations in angiosperms, with up to 95% of all auxin in a plant bound into one of these storage forms (Cohen and Bandurski 1982; Bandurski and others 1995; Campanella and others 1996; Walz and others 2002).

The ILR1-like auxin amidohydrolase gene family was initially characterized in *Arabidopsis thaliana* (Bartel and Fink 1995; Davies and others 1999; LeClere and others 2002) and is thought to be involved in regulation of free IAA. The first enzyme isolated in this family, ILR1, cleaves IAA-Leu and IAA-Phe preferentially, whereas the ILL1, ILL2, and IAR3 enzymes prefer IAA-Ala as a substrate. The closely related sILR1 ortholog, isolated from *Arabidopsis suecica*, has substrate specificity for IAA-Gly and IAA-Ala (Campanella and others 2003a, 2003c). Active amidohydrolase orthologs (BrILL2 and BrIAR3) have also been isolated from *Brassica rapa* (Schuller and Ludwig-Müller 2006). In addition, a novel conjugate hydrolase has been characterized in wheat that has little specificity for IAA conjugates but hydrolyzes conjugates of IBA and indole-3-propionic acid (IPA) (Campanella and others 2004).

We chose *Medicago* as our model system because it is a legume that can be induced in plant-microbe interactions to undergo both nodulation and AM formation (Cook and others 1997). Moreover, phylogenetic studies had determined that *Medicago* has a large family of putative auxin conjugate hydrolases (Campanella and others 2003b). In addition, several expressed sequence tags (ESTs) for two of the putative hydrolase genes described above were found in cDNA libraries from mycorrhizal roots (unpublished observations), suggesting an increase in hydrolase expression during AM formation. Finally, microarray hybridization analyses showed some overlap of auxin-inducible and AM-inducible genes in *Medicago* roots (J. Ludwig-Müller, unpublished data), and several AM-inducible genes were also inducible by IAA or IBA (Ludwig-Müller and Güther 2007). This evidence supported the hypothesis that surges in auxin may be involved in early symbiotic interactions in *Medicago*. Given this information our goal was to determine whether the *MtIAR3* gene family was involved in regulating auxin homeostasis during AM symbiosis and whether this regulation could be observed during the nodulation process.

In this article we report on the isolation, expression analysis, and enzymatic characterization of five putative auxin amidohydrolases (MtIAR31, MtIAR32, MtIAR33, MtIAR34, and MtIAR36) with homology to the *Arabidopsis* ILR1-like family. We found the members of this family to be diverse in their hydrolase activity, substrate specificity, and spatiotemporal expression. More importantly, a subset of hydrolase transcripts seems to be exceedingly upregulated during the first 1–15 days of rhizobia-induced nodulation, whereas they are only

moderately induced during fungal-induced AM formation. Finally, we report an IBA increase in *Medicago* during AM formation.

Materials and Methods

Plant Materials and Plant Growth

Medicago truncatula (Jemalong A17) seeds were scarified by scraping gently on an emery board. Seeds were then incubated in 2–3 ml of 30% bleach and 0.1% Triton X-100. Seeds were washed 2–3 times in 1–2 ml of sterile water and then imbibed and incubated for 2–3 days at 4°C in darkness.

Seeds used for sources of root, leaf, stem, and flower tissue were first germinated on sterile minimal media 2% agar [5 mM KNO_3, 2.5 mM K_2HPO_4 (pH 5.5), 2 mM $MgSO_4$, 2 mM $Ca(NO_3)_2.H_2O$, 50 μM Fe-EDTA, 70 μM H_3BO_3, 14 μM $MnCl_2$, 0.5 μM $CuSO_4$, 1 μM $ZnSO_4$, 0.2 μM $Na_2MoO_4{\cdot}2H_2O$, 10 μM NaCl, 0.01 μM $CoCl_2$]. Once germinated, the seedlings were sown in soil (perlite:sphagnum peat moss:vermiculite, 1:1:1 v/v/v) saturated with liquid minimal medium. Plants were slowly hardened off over one week and fertilized with liquid minimal medium every week as needed. The plants were grown at 23°C in constant light (cool white, fluorescent, ~100 μmol s^{-1} m^{-2}) in a plant growth chamber (Percival Scientific, Model E-30B).

Leaves, roots, and stems for spatial expression analysis were harvested 20 days after germination. Flowers were harvested at 74 days after germination. All tissues were stored frozen at -80°C until RNA extraction.

Seeds used for developmental expression studies were germinated on sterile agar medium and transferred to soil after germination. The plants were grown at 23°C in constant light (cool white, fluorescent, ~100 μmol s^{-1} m^{-2}) in a plant growth chamber (Percival Scientific, Model E-30B). Whole seedlings were collected 1, 5, 10, and 20 days after germination and stored frozen at -80°C until RNA extraction.

Scarified, sterilized, and washed *Medicago* seeds used in the root nodulation experiment were transferred to buffered nodulation medium with 1 nM β-aminoisobutyric acid (Ehrhardt and others 1992). Seeds were incubated 3 days in the dark at 4°C and then transferred to the plant growth chamber at 23°C with 14 h of light per day at approximately 100 μmol s^{-1} m^{-2}. Five days after germination the seedlings were exposed to the rhizobia.

Induction of Nodulation

Sinorhizobium meliloti strain 1021 was grown overnight in liquid LB media with constant shaking, 200 rpm, at 28°C. The OD_{600} of the overnight culture was found to be 0.6, which is acceptable for induction (Ehrhardt and others 1992). Two milliliters of bacteria were centrifuged at 5000 rpm and washed 3 times in 2 ml of fresh liquid LB media. The cells were resuspended in 10 ml liquid LB media and added to the Petri dishes containing the 5-day-old *Medicago* seedlings. For mock infection, seedlings were treated with distilled water. The *Medicago* roots were incubated 5 min at room temperature with the bacterial culture. The bacteria were pipetted away, and the "0" day tissue was cut from treated and mock-infected plants and frozen at –80°C immediately for later RNA extraction. The rest of the plants, remaining on agar, were returned to the plant growth chamber at 23°C with 14 h of light per day at approximately 100 μmol s^{-1} m^{-2} and roots were harvested at days 1, 2, 5, 10, and 15 after germination.

AM Inoculation

Seedlings of *Medicago* were cultivated under sterile conditions as previously described in a plant growth chamber (Percival Scientific, Model E-30B) at 25°C with a photoperiod of 15 h light:9 h dark. The *Glomus intraradices* inoculum was obtained commercially (Reforestation Technologies International, Salinas, CA). Seedlings were transplanted to soil (perlite:sphagnum peat moss:vermiculite, 1:1:1 v/v/v) saturated with liquid minimal medium and inoculated with approximately 20,000 propagules of sterile AM fungi after the root and coleoptile tips were visible (8 days after germination on MSO agar). Mock-infected seedlings were germinated sterilely in the same fashion as described above and transferred separately to soil untreated by AM fungi.

The "0" day root tissue was cut from treated and mock-infected plants and frozen at –80°C immediately for later RNA extraction. The rest of the plants were returned to the growth chamber at 25°C with 15 h of light per day at approximately 100 μmol s^{-1} m^{-2}, and roots were harvested at days 5, 10, 15, and 21 after inoculation with *Glomus*. The percentage of root length colonized was determined by counting the fungal structures (hyphae, arbuscules, vesicles) in infected roots after staining with lactophenol blue as described earlier (Schmitz and others 1991).

RNA Extraction

Total RNA was extracted from approximately 0.4 g of plant tissue, using the RNeasy RNA extraction kit (Qiagen, Valencia, CA). Before extraction, micropestles and all microfuge tubes were treated with an 8% solution of RNA Secure (Ambion Corporation, Austin, TX) for 10 min at

65°C. RNA concentration was determined by UV absorbance in a NanoDrop model ND–1000 spectrophotometer (NanoDrop Technologies, Wilmington, DE) and samples were stored at –80°C as separate aliquots until real-time reverse transcriptase PCR (RT-PCR) analysis could be performed.

Cloning of Full-Length *MtIAR3* Family of cDNAs

The cDNA sequences for *MtIAR31*, *–32*, *–33*, *–34*, and *–36* (*Medicago* TIGR Accession Nos. TC77457, TC77458, TC87843, TC79815, TC102108, respectively) were obtained from The Institute for Genomic Research (TIGR) sequence database and first identified as an *IAR3* ortholog using TIGRBLAST (Altschul and others 1990).

Total *Medicago* mRNA was extracted from whole seedlings and RT-PCR was then used to amplify the specific cDNA of *MtIAR31*, *–32*, *–33*, *–34*, and *–36*. The transcript primers employed to amplify the *MtIAR3* family are listed in Table 1. Single 50-µl reactions were carried out in an RNase-free 0.5-ml microfuge tube using an Eppendorf Mastercycler gradient thermocycler (Eppendorf, Inc., Westbury, NY). The reverse transcriptase reaction was incubated at 50°C for 1 h, followed by 95°C for 15 min. The PCR step was performed for 36 cycles at the following times and temperatures: 45 s at 95°C, 45 s at 57°C, and 1 min at 72°C.

The resulting amplified cDNA was blunt-end ligated in-frame into the EcoRV cloning site of the pETBlue-2 expression vector (Novagen Corp., San Diego, CA) using T4 DNA ligase (Novagen) in such a way that the cDNA was terminated by its own stop codon and the His-Tag of the pETBlue-2 vector was not expressed. The resulting constructs (peMtIAR31, peMtIAR32, peMtIAR33, peMtIAR34, peMtIAR36) were then transformed into *E. coli* (NovaBlue) using heat shock (Sambrook and others 1989) and putative transformants were selected on the basis of ampicillin resistance and blue-white selection (Sambrook and others 1989). Plasmids were obtained from transformants by alkaline lysis (Sambrook and others 1989). Insert orientation and size were determined by endonuclease digestion, electrophoretic analyses through 1% agarose gels, and DNA sequencing of the insert regions using BigDye Terminator version 3.0 (Applied Biosystems, Foster City, CA) on an ABI model 3730 DNA analyzer following the manufacturer's directions.

Real-Time RT-PCR

The primers employed to amplify *MtIAR31*, *–32*, *–33*, *–34*, and *–36* for expression analysis are listed in Table 1. For the expression analyses, single 500-ng, 25-µl reactions were carried out in RNase-free 0.2-ml microfuge tubes using an Mx3000p Real Time Thermocycler (Stratagene, La Jolla, CA). The iScript One-Step RT-PCR kit with SYBR Green (Bio-Rad, Laboratories, Hercules, CA) was used according to the manufacturer's instructions to amplify the specific cDNA of *MtIAR31*, *–32*, *–33*, *–34*, and *–36*. The reverse transcriptase reaction was incubated at 50°C for 1 h, followed by 95°C for 15 min. The PCR step was performed for 40 cycles at the following times and temperatures: 45 s at 95°C, 45 s at 57°C, and 1 min at 72°C. Each experiment was replicated three times and values averaged. 18S RNA was used as an expression control.

The bar graphs indicating hydrolase transcript expression were generated from the real-time RT-PCR data using the standard curve method described by Applied Biosystems (User Bulletin No. 2, ABI Prism 7700 Sequence Detection System; http://www.appliedbiosystems.com) using MX3000P software (Stratagene). In this method product amounts were normalized to the 18S standard and a relative standard curve was generated using a basis sample called

Table 1 Primers used to RT-PCR amplify cDNA of hydrolase genes for cloning (A) and real-time RT-PCR analysis of transcript expression (B)

Allele	Forward primer	Reverse primer
MtIAR31	(A) 5′-TTTTCTTTCTTTTCCATTTCTC-3′	5′-TAAATAATATTTGCTTATAA-3′
	(B) 5′-TTATCACTGGACAAGCTGCTG-3′	5′-TTATAATTCATCATGAATTTTCCCCTTT-3′
MtIAR32	(A) 5′-TTCAATACCTTGAGAGCATCCATCC-3′	5’-ACAACACAAAGGGCTAGGGA-3′
	(B)5′-GATGGTGGCTTGCATGACTA-3′	5′-ACAACACAAAGGGCTAGGGA-3′
MtIAR33	(A) 5′-ACGAGTGGCTTGGAAGTTAAA-3′	5′-CGTTTCAATTTTACATTTTCTTCG-3′
	(B) 5′-AGGAGCCAGACAACGGAAG-3′	5′-CATGATACATCAGTAATAACAAAAGG-3′
MtIAR34	(A) 5′-TGCTTCAATCATCAACCTTCA-3′	5′-TGATGAAACCAGAGTATGTAGTGAAA-3′
	(B) 5′-TGCTTCAATCATCAACCTTCA-3′	5′-ATTGGACCAGACCTGGAGGA-3′
MtIAR36	(A) 5′-TGTTCCTTGCTTTGCTTCAT-3′	5′-TGGTTTCCGAGATCAACCAT-3′
	(B) 5′-TACCCTCCCACGGTTAATGA-3′	5′-TGGTTTCCGAGATCAACCAT-3′

a calibrator. For all experimental samples target quantity was determined from the standard curve and divided by the target quantity of the calibrator. The calibrator acted as the 1× sample and all other samples were expressed in differences relative to the calibrator.

Enzyme Preparation from *E. coli*

The peMtIAR31, –32, –33, –34, and –36 strains (containing the *Medicago* homologs of *IAR3* in the EcoRV site of the pETBlue–2 vector) were grown overnight in 5 ml LB medium containing 100 μg/ml ampicillin. From this culture 2 ml were transferred to a flask containing 50 ml LB medium, including 100 μg/ml ampicillin and 1 mM IPTG for gene induction. Induction was performed for 4 h with continuous shaking of the cultures. Uninduced controls were grown under the same conditions but without IPTG. Instead, 0.5% glucose was included in the medium because the promoter of pETBlue-2 is leaky.

Enzyme preparation and enzymatic activity assays were conducted as in our previous studies (Campanella and others 2003c, 2004). After collecting the bacterial cells by centrifugation for 10 min at 8000*g*, the pellet was resuspended in 100 μl lysozyme buffer per initial 1 ml bacterial culture (30 mM Tris-HCl, pH 8.0, containing 1 mM EDTA, 20% sucrose, and 1 mg/ml lysozyme, Sigma-Aldrich, St. Louis, MO) for cell lysis and incubated for 10 min at 4°C. To break the cells, three freeze-thaw cycles were performed where the cells were frozen in liquid N_2 and thawed at 30°C. After the last thawing, 2 μl of a 10-mg/ml DNase solution in 150 mM NaCl and 50% glycerol was added and the mixture was incubated for 15 min at 25°C. The extract (100 μl volume per assay) was then directly used for the enzyme assay.

Enzyme Assay with MtIAR3 Family

The enzyme assay for the hydrolysis of auxin conjugates was performed in a 500-μl reaction mixture containing 395 μl assay buffer, 100 μl bacterial enzyme extract (corresponding to approximately 2.5 mg total protein), and 5 μl of a 10 mM stock solution (dissolved in a small volume of ethanol, then diluted with H_2O) of each substrate (final concentration 100 μM; ethanol concentration was always $< 0.1\%$). The substrates used in this study were the IAA amide conjugates IAA-Asp, IAA-Ala, IAA-Gly, IAA-Leu, IAA-Ile, IAA-Phe, and IAA-Val (all from Sigma), the IAA ester conjugate IAA-glucose (a gift from Dr. Jerry D. Cohen), and the amide conjugates of IBA with alanine (Sigma) and glycine, the latter obtained after demethylation of methyl-IBA-Gly (a gift from Dr. Joseph Riov; Campanella and others 2004). The assay buffer consisted of 100 mM Tris, pH 8.0, 10 mM $MgCl_2$, 100 μM $MnCl_2$, 50 mM KCl, 100 μM PMSF, 1 mM DTT, and 10% sucrose (Ludwig-Müller and others 1996) however, for the assays that included IAA-Asp as substrate, no DTT was added. The reaction was incubated for 1 h at 40°C, stopped by adding 100 μl 1 N HCl, and the aqueous phase was then extracted with 600 μl ethyl acetate. The organic phase was removed, evaporated to dryness, and resuspended in 100 μl CH_3OH for HPLC analysis according to Campanella and others (2004). The experiments were repeated 3-4 times using different enzyme preparations. All results represent means of independent experiments ± standard error (SE). The uninduced cultures were evaluated as controls. The enzymatic activity was calculated as nanomoles of IAA released from cultures induced with IPTG subtracted by the values obtained in noninduced cultures.

Auxin Determination

Medicago roots inoculated with *Glomus intraradices* were harvested at different time points during the colonization process. Control roots were harvested at the same age. A minimum of 0.1 g fresh weight per individual analysis was extracted with a mixture of isopropanol and acetic acid (95:5 v/v). To each sample 100 ng $^{13}C_6$-IAA (Cambridge Isotope Laboratories, Andover, MA) and 100 ng $^{13}C_1$-IBA (a gift from Dr. E. Sutter; Sutter and Cohen 1992) were added. Sample preparation was performed according to Meixner and others (2005). Derivatization of samples was performed by methylation according to Cohen (1984) with freshly prepared diazomethane. GC-MS analysis was carried out on a Varian Saturn 2100 ion-trap mass spectrometer using electron impact ionization at 70 eV. The spectrometer was connected to a Varian CP-3900 gas chromatograph equipped with a CP-8400 autosampler (Varian, Darmstadt, Germany). For the analysis 2.5 μl of the methylated sample dissolved in 20 μl ethyl acetate was injected in the splitless mode (splitter opening 1:100 after 1 min) onto a Phenomenex ZB-5 column (Aschaffenburg, Germany), 30 m × 0.25 mm × 0.25 μm, using He carrier gas at 1 ml min^{-1}. Injector temperature was 250°C and the temperature program was 60°C for 1 min, followed by an increase of 25°C min^{-1} to 180°C, 5°C min^{-1} to 250°C, 25°C min^{-1} to 280°C, then 5 min isothermically at 280°C. Transfer line temperature was 280°C and the trap temperature was 200°C. For higher sensitivity, the μSIS mode (Varian Manual; Wells and Huston 1995) was used. For the determination of IAA and IBA, the quinolinium ions of the methylated

substance derived from endogenous and $^{13}C_6$-IAA and $^{13}C_1$-IBA at *m/z* 130/136 and 130/131, respectively, were monitored (Ludwig-Müller and Cohen 2002). The endogenous hormone levels were calculated by the principles of isotope dilution (Cohen and others 1986).

Phylogenetic Tree Construction and Chromosomal Linkage

Amino acid alignments of the MtIAR3 family and the *Arabidopsis* orthologs were performed using the ClustalX v1.8 software (Thompson and others 1997). Alignment settings were used at default values. Phylogenetic trees were generated from the distances provided by the ClustalX analysis using the neighbor-joining method (Saitou and Nei 1987). Bootstrap analyses (Felsenstein 1985) consisted of 1000 replicates. The neighbor-joining trees were visualized with the TREEVIEW program (Page 1996). The protein sequence of a bacterial M20 peptidase from *Campylobacter jejuni* (GenBank accession No. Z36940) was used as an outgroup.

The chromosomal linkage groups for the hydrolase loci were determined by cDNA homology searches on the NSF/EU *Medicago truncatula* Sequencing Resources web page at http://www.medicago.org/genome.

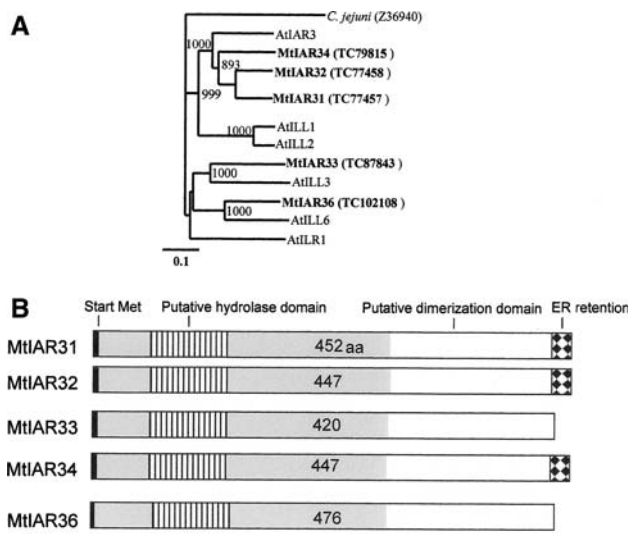

Fig. 1 **A** Neighbor-joining phylogram of *Arabidopsis thaliana* ILR1-like protein family members orthologous to the *MtIAR3* family. The TIGR accession numbers are indicated for each *Medicago* gene, and the scale at the bottom of the figure indicates relative genetic distance. Bootstrap values out of 1000 are indicated on the nodes of the tree. **B** Schematic overview comparison of the putative protein structures of the five *Medicago* hydrolases. The numbers indicate the number of amino acid residues of the respective protein. The lined boxes are the putative active sites, the white boxes are the putative dimerization sites, and the hatched boxes on MtIAR31, –32, and –34 represent the endoplasmic reticulum retention signal. aa = amino acid

Results

Phylogenetic Analysis of an Auxin Amidohydrolase Family in *Medicago truncatula*

A phylogenetic analysis comparing the MtIAR3 family of proteins against all the members of the ILR1-like family confirms that the majority (MtIAR31, –32, and –34) are similar to AtIAR3 (Figure 1a), with a clade bootstrap value of 1000. The MtIAR33 homolog appears to be most closely related to the *Arabidopsis* ILL3 protein, whereas MtIAR36 is most similar to AtILL6. The MtIAR31, –32, and –34 products contain putative C-terminal endoplasmic reticulum (ER) retention signals (Figure 1b), a hallmark of many of the auxin amidohydrolases (Davies and others 1999; LeClere and others 2002; Campanella and others 2003a, 2003b, 2004). In addition, analyses employing the Pence Proteome Subcellular Localization Server v2.5 (Lu and others 2004) demonstrated that all five *Medicago* hydrolases studied contain putative N-terminal ER localization signals (data not shown), which are basically homologous to those found in AtILR1 or AtILL2 proteins.

We have been able to determine the putative chromosomal locations for all five hydrolase genes by using data from the *Medicago truncatula* genome sequencing projects. *MtIAR31* seems to be homologous to the Mth2-145C3 clone linked to *Medicago* Chromosome 8 at approximately position 44. *MtIAR32* appears be linked to *Medicago* Chromosome 2 at position 64. *MtIAR33* appears

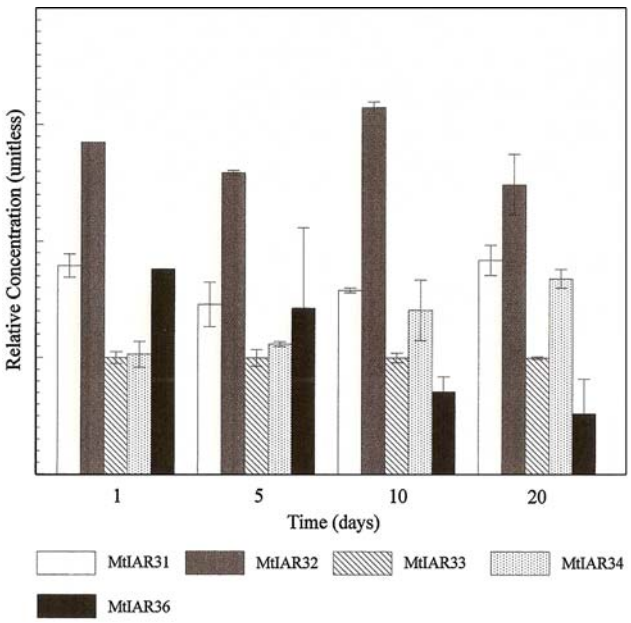

Fig. 2 Whole-plant relative temporal expression of *MtIAR3* transcripts given in days after germination. The calibrator was the *MtIAR33* expression data. The data are the average of three experiments ± SEM

on Chromosome 3 at position 84.3, as does *MtIAR34* at position 70.8. Computer analysis of *MtIAR36* found it to have 100% homology to a portion of the Mth2-12B2 clone also on Chromosome 3 at approximately position 63.7.

Temporal and Spatial Expression of the *MtIAR3* Gene Family

All transcripts are detectable in whole seedlings at day 1 after germination (Figure 2). The *MtIAR32* mRNA consistently appears to be at the highest level of expression for the 20-day period in whole seedlings, whereas *MtIAR33* appears to be consistently expressed at a low level. *MtIAR31* and *–34* decrease into a midrange value of expression between *MtIAR32* and *MtIAR33. MtIAR36* is expressed at a midrange value at day 1, but expression reduces to the lowest compared to the other family members by day 20.

With the exception of *MtIAR36*, there seems to be little fluctuation in expression in any of the family members, with only small changes in mRNA concentrations observable over time. It is unclear which, if any, of these products may be important for generalized early growth, although the high and regular level of *MtIAR32* makes it the most likely candidate. Expression of the 18S control showed no difference between samples examined (data not shown).

The relative spatial expression of all the homologs in various plant tissues was determined (Figure 3). The *MtIAR32* transcript appears to be expressed at the highest level of any family member in lower leaves, stem, and root, whereas *MtIAR31* is the highest of the family in flower tissue. *MtIAR36* transcript was expressed most strongly in upper leaves with high concentrations in stem tissues as well.

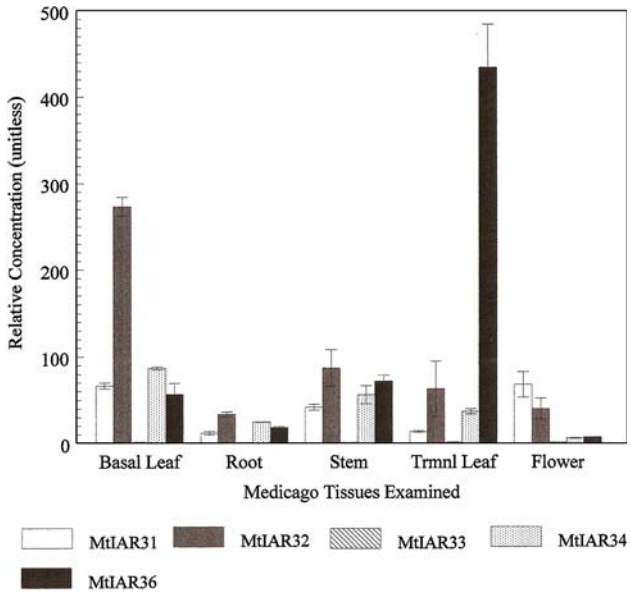

Fig. 3 Relative expression of *MtIAR3* transcripts in each plant tissue. The calibrator was the *MtIAR33* expression data. The data are the average of three experiments ± SEM

The *MtIAR33* transcript was expressed at the lowest relative level compared to all other *Medicago* homologs in every tissue examined. Note that *MtIAR33 is* being expressed, despite its apparent exclusion in the study (Figure 3). This analysis reflects relative expression. *MtIAR33* is expressed the least in all the tissues examined, so it was set by the Stratagene MX3000P software as the baseline comparator of "1×" in the experiment against which all other expression was evaluated, and hence it appears apparently unseen in Figure 3 against the much greater expression of the other homologs.

Presumably the upregulated gene products are needed for specific growth and development of the particular tissues studied. Expression of the 18S control showed no difference between samples examined (data not shown).

MtIAR3 Gene Family Expression During Nodulation

At 15 days after inoculation, the visual onset of root nodule formation was observed in all infected roots (data not shown). During the 15 days of bacterial invasion by *Sinorhizobium meliloti* in *Medicago*, the expression of *MtIAR32* and *–36* transcripts showed little variation above the mock-control values (Figure 4a, b). *MtIAR31* demonstrated slight expression increases of approximately 18-fold by day 5; this result may support the hydrolase as a potential maintenance factor in the later stages of nodulation. In sharp contrast, *MtIAR33* and *–34* were highly upregulated (∼2500-fold and 165-fold, respectively) at the very early stages of nodulation induction (Figure 4a). The expression of *MtIAR33* increased rapidly by day 1 after bacterial inoculation and then decreased by day 15, although it was still tenfold higher than the day 0 comparator (Figure 4a). In all cases of upregulation, the infected tissues demonstrated a clearly increased expression compared to mock-infected tissues (Figure 4b). Expression of the 18S control showed no difference between samples examined (data not shown).

MtIAR3 Gene Family Expression During Arbuscular Mycorrhiza Formation

During the 21 days of fungal colonization of *Medicago* with *Glomus intraradices*, expression of the *MtIAR31* and *–36* transcripts changed little (Figure 5). The *MtIAR32* transcripts demonstrated an induction increase of approximately fourfold by day 10 after inoculation. The strongest

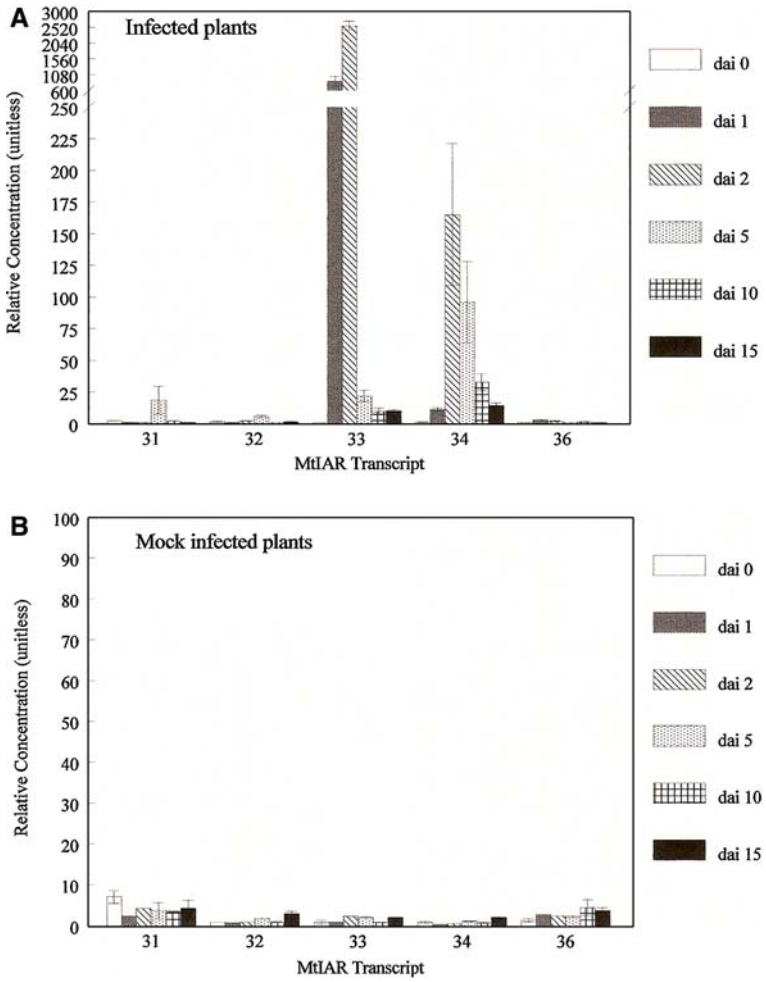

Fig. 4 Relative expression of the *MtIAR3* family in root tissues during nodulation. **A** Hydrolase transcript expression in roots infected with *Sinorhizobium* bacteria. The infected roots are designated as 31, 32, 33, 34, and 36 indicating the appropriate *MtIAR3* family member. **B** Hydrolase transcript expression in the mock-infected control roots. The data are the average of three experiments ± SEM; dai = days after inoculation

inductive effects were seen in *MtIAR33* and *–34*, which were moderately upregulated to approximately 14-fold and approximately tenfold by day 10, respectively (Figure 5). In all cases of upregulation, the AM inoculated tissues demonstrated an increased expression compared to mock-infected tissues (data not shown). Expression of the 18S showed no difference between samples examined (data not shown). Mycorrhizal colonization started between 5 and 7 days after inoculation with 7% and 2%, respectively, and reached up to 60% at 42 days after inoculation in the different experiments (Figures 5, 6). Therefore, the increase in *MtIAR3* transcripts correlated with an early onset of colonization. During the time points of increased *MtIAR3* expression, mainly intraradical hyphae were present and only an occasional arbuscule was spotted (data not shown).

The levels of free IBA were constantly increased during the development of the symbiosis with *Glomus intraradices* over a period of 7–42 days after inoculation. The onset of the IBA increase correlates with the increase in auxin conjugate hydrolase transcripts of *MtIAR33* and *–34*. In contrast, free IAA levels were only transiently increased at one time point (Figure 6). To our knowledge it was the first time that IBA was demonstrated by full-scan GC-MS to be present in the species *Medicago* (data not shown).

Substrate Specificity of the *MtIAR3* Gene Family

Are all of the differentially expressed hydrolases active? After cloning the cDNAs of *MtIAR31*, *–32*, *–33*, *–34*, and *–36* (GenBank accession Nos. DQ489992, DQ489993, DQ489994, DQ489995, DQ489996, respectively) into pETBlue-2, the enzyme activity was determined *in vitro* (Table 2). Enzyme activity from cells containing an empty vector was compared with that from cells containing the peMtIAR31, –32, –33, –34, and –36 vectors. These cells were either incubated with glucose because the promoter from pETBlue-2 is leaky or induced with isopropyl *β*-thiogalactopyranoside (IPTG).

Although MtIAR31, –32, –33, and –34 are all able to hydrolyze IAA-Asp well, MtIAR33 has the strongest activity against IAA-Asp, with 1160 ± 80 pmol auxin released/min/ml (Table 2). MtIAR33, –34, and –36 strongly hydrolyze the ester bonds of IAA-glucose.

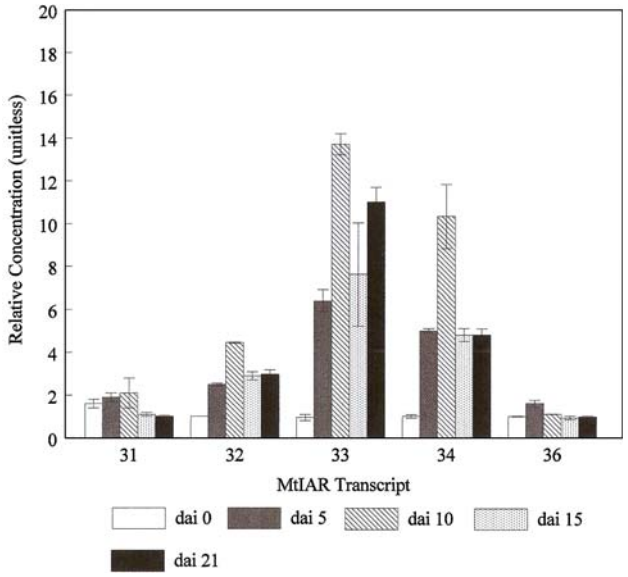

Fig. 5 Relative expression of the *MtIAR3* family in root tissues during AM colonization. The infected roots are designated as 31, 32, 33, 34, and 36 indicating the appropriate *MtIAR3* family member at the time point (days) after inoculation (dai). The data are the average of three experiments ± SEM. In all cases of upregulation, the AM-inoculated tissues demonstrated an increased expression compared to mock-infected tissues (data not shown). Mycorrhization rates were 0 dai = 0%; 5 dai = 7%; 10 dai = 15%; 15 dai = 18%; 21 dai = 32%

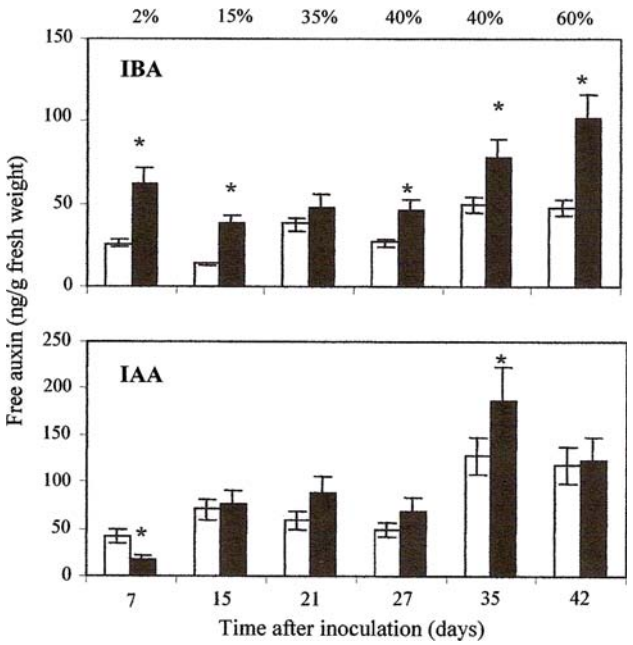

Fig. 6 Free auxin levels in *Medicago truncatula* control roots (□) and roots after inoculation with *Glomus intraradices* (■). Mean values ± SE are presented. The values consist of three independent biological experiments, and for each experiment three technical replicates were performed. The asterisk indicates significance at the $p \leq 0.05$ level. The percent values above the upper panel represent the total AM colonization rates

MtIAR34 appears to have the most overlapping activity of any of the other hydrolases, being able to hydrolyze IAA amide, ester, and IBA conjugates. MtIAR36 is the only member of this family with high activity against IAA-Gly, -Ile, and -Ala (Table 2).

One feature of the MtIAR3 family hydrolases –31, –32, –33, and –34 is their ability to cleave IAA-Asp (Table 2). The *Arabidopsis thaliana* and *A. suecica* hydrolases were not able to accept IAA-Asp as substrate (LeClere and others 2002; Campanella and others 2003c), but a bacterial hydrolase from *Enterobacter agglomerans* was able to hydrolyze IAA-Asp with high substrate specificity (Chou and others 1998, 2004). This activity was inhibited by dithiothreitol (DTT) (Chou and others 1998), whereas the activity of plant hydrolases was generally dependent on the presence of DTT (data not shown). Because several *E. coli* strains also hydrolyze IAA-Asp to some extent, we have carefully examined the IAA-Asp hydrolyzing activity of the strain (NovaBlue) used in this study and found very little activity of (1) the bacterial strain without plasmid, (2) bacteria with empty vector, and (3) bacteria where the promoter was suppressed with glucose so that no protein could be formed (data not shown). Only when the *E. coli* cells were induced with IPTG was a significant amount of IAA-Asp hydrolyzed. We have also tested whether DTT inhibits the IAA-Asp hydrolyzing activity of the *Medicago* enzymes. MtIAR31 and MtIAR32 were indeed inhibited by DTT and the IAA-Asp hydrolysis activity was reduced by about 80% and 90%, respectively. Using DISULFIND (Cysteines Disulfide Bonding State and Connectivity Predictor) (Ceroni and others 2003; Vullo and Frasconi 2004), we predicted that the conserved cysteines do not form double bonds within the molecule. However, the possibility that the proteins form homodimers must be further investigated.

Recent X-ray crystallography studies have suggested that the AtILR1 auxin amidohydrolase contains a putative exopeptidase dimerization domain in its tail region (Structural Classification of Protein Database, accession No. 117980) that is conserved from bacterial hydrolases. Our own analyses indicate that these same homologous dimer domains can be found in all the *Medicago* hydrolases described here. Although dimerization has been demonstrated in bacterial systems for prokaryotic hydrolase orthologs (Structural Classification of Protein Database, accession Nos. 55034, 103002, and 75444), there is still no evidence of formation of dimers in plant hydrolases.

Discussion

Auxin conjugates play an important role in controlling auxin homeostasis. Their synthesis and hydrolysis must be

Table 2 Enzyme activity of the five *MtIAR3* homologs

Substrate	Enzyme activity (pmol auxin released/min/ml)[a]				
	MtIAR31[*]	*MtIAR32*[*]	*MtIAR33*[**]	*MtIAR34*[**]	*MtIAR36*[*]
IAA-Ala	0	40 ± 11	50 ± 10	50 ± 13	**220 ± 85**
IAA-Gly	0	10 ± 2	80 ± 7	30 ± 5	**1030 ± 348**
IAA-Phe	0	**5 ± 1**	0	0	0
IAA-Asp	430 ± 20	840 ± 40	**1160 ± 80**	500 ± 123	0
IAA-Leu	0	0	0	**70 ± 18**	0
IAA-Ile	0	0	0	0	**410 ± 68**
IAA-Val	16 ± 4	0	0	**20 ± 3**	0
IAA-glucose	24 ± 0.5	0	160 ± 19	240 ± 46	**390 ± 29**
IBA-Ala	**680 ± 90**	140 ± 30	60 ± 9	270 ± 29	10 ± 3
IBA-Gly	0	**20 ± 6**	10 ± 2	0	0

[a] Activity in pmol auxin/min/ml *E. coli* extract. Mean values of three (*) to four (**) independent experiments are given. Bold values indicate strongest activity against the respective substrate.

regulated throughout plant development to control free auxin levels. Therefore, understanding regulatory mechanisms of auxin conjugate hydrolysis is of interest. We have isolated five auxin conjugate hydrolases from the species *Medicago truncatula*, which is a good model system for the investigation of various symbiotic interactions. We have found that these enzymes have overlapping, but distinct, hydrolytic enzymatic activities against a variety of IBA and IAA conjugate substrates. Those proteins whose genes are induced during symbiotic interactions might therefore be suitable candidates to be involved in the regulation of auxin homeostasis during the two root symbioses examined.

Although we believe our observations on "overlapping" enzymatic activities to be physiologically important, an alternative view has been suggested by other researchers (Jensen 1976; James and Tawfik 2001; Roodveldt and Tawfik 2005), that "promiscuous activities" in the amidohydrolase superfamily may be part of their evolutionary "accessories" that allow directed evolution. This promiscuity would permit structurally related enzymes with common motifs, like the ubiquitous "TIM-barrel" fold in the amidohydrolases, to have a variety of different minor enzymatic functions, such as esterase, with an assortment of substrates that could develop into primary functions under the correct physio-environmental conditions. One concern, in our own observations, is how the apparent esterase/acyl anhydride activity seen in MtIAR33, –34, and –36 is related to the concomitant amidohydrolase activity. One might argue that the observed esterase cleavage of IAA-glucose may be a minor activity, whereas the amidohydrolase activity is actually primary. Such shared, overlapping activities may reflect their functions as "node intermediates" along future evolutionary pathways in *Medicago* and may not embody principal enzymatic functions.

We do not think that the observed activity against IAA-glucose described here is the result of a nonspecific chemical breakdown of the sugar conjugate such as observed by Baldi and others (1989). We conducted a comparison between the activity measured in cells that were not induced and the activity in cells that were induced by IPTG to form the enzyme. Therefore, nonspecific hydrolytic activities that may occur at mild alkaline pH values above 7 (Baldi and others 1989) or other nonenzymatic processes have been subtracted from the actual enzymatic activity. In addition, the incubation time was only 1 h, which was below the periods given by Baldi and others (1989). However, whether this *in vitro* activity really reflects the enzymatic activity *in planta* has yet to be determined.

In addition to the enzymatic activity, we have examined expression of this family of hydrolases both spatially and temporally. We have found that MtIAR32 is the hydrolase expressed at the highest level during the period between germination and 20 days of age. Because MtIAR32 has high enzymatic activity against an IAA conjugate (IAA-Asp) in the MtIAR3 family (Table 2) and is upregulated during growth (Figure 2), it is likely that this enzyme is important in regulating the release of free IAA during general developmental processes. MtIAR31 may play a secondary, redundant role during development because it is expressed at the second highest level over the first 20 days of growth, and it also has strong hydrolase activity against IAA-Asp.

MtIAR32 may be the primary hydrolase involved in general growth responses because it is expressed spatially at the highest levels of any hydrolase in most tissues examined (lower leaves, roots, and stems) (Figure 3). All the hydrolase transcripts, except *MtIAR33*, are expressed at the same levels in stem tissue, which would be a primary

location for auxin release and intense growth in a herbaceous plant such as *Medicago* (Figure 3). This result supports overlapping functional redundancy, such as that observed in the ILR-like family in *Arabidopsis* (Rampey and others 2004).

MtIAR36 is highly expressed in the terminal leaf (Figure 3). This was the only tissue or condition that we have examined so far where this specific isoform was more highly expressed than all the other hydrolase transcripts. Together with its dissimilar substrate specificity, this hydrolase might play a distinct function in *Medicago* development. It is interesting to note that two active *Medicago* hydrolases (MtIAR33 and –36) are more homologous to *Arabidopsis* hydrolases ILL3 and ILL6, respectively, for which no catalytic activities have been described so far (Davies and others 1999). It has not been possible to test the expression of another full-length ILL6 homolog from *Brassica rapa* for comparable enzymatic activity because predicted transmembrane domains have possibly prevented its expression in *E. coli* (Schuller and Ludwig-Müller 2006).

One of the primary goals of this study was to determine whether any of the members of this hydrolase family were upregulated during induction of the process of rhizobial nodulation or AM formation. From our results it appears that a subset of hydrolase transcripts are upregulated during both nodulation and AM formation, thus possibly leading to elevated auxin levels. Although IAA might be necessary to induce the primordia after-infection with rhizobia, leading to root nodule formation (Hirsch and others 1997), elevated auxin levels might lead to an altered root morphology after AM colonization (Kaldorf and Ludwig-Müller 2000).

Altered auxin levels might not only determine the morphology of organs/nodules during symbiosis but may also be involved in a phenomenon called "autoregulation" (Meixner and others 2005), that is, already existing nodules or an existing root colonization by an arbuscular mycorrhizal fungus systemically suppresses subsequent nodule formation/root colonization in other parts of the root system (Caetano-Anollés and Gresshoff 1991; Vierheilig 2004).

During the initial process of nodulation over the first 48 h, only the MtIAR33 and –34 transcripts were upregulated (Figure 4). We may hypothesize that among these putative regulatory enzymes, MtIAR33 may be particularly important for releasing auxin from the conjugated state during the early process of nodulation. MtIAR33 has very strong enzymatic activity against IAA-Asp, which is one of the most commonly observed conjugates found in dicots (Bartel and Fink 1995; LeClere and others 2002; Rampey and others 2004). MtIAR34 may also be very important in early nodulation because it has demonstrated the widest hydrolytic activity against different substrates and the MtIAR34 transcript is upregulated almost 175-fold during nodulation. However, a correlation between the potential increase in free IAA or IBA during nodulation and the hydrolase transcript has yet to be shown.

It has been shown in different host plants, among them *Medicago truncatula*, that auxin accumulation is taking place at the site of nodule formation (Mathesius and others 1998; Pacios-Bras and others 2003; Huo and others 2006). However, no such data are found for AM-colonized *Medicago* roots. We therefore measured IAA and IBA levels in control and *G. intraradices*-inoculated roots over a time course of AM development. Free IBA increased during early time points of colonization in *Medicago* roots, remaining elevated compared to control roots for the rest of the investigated time period (Figure 6). The early rise in IBA correlates with an increase of several hydrolase transcripts during the early stages of AM formation, where the predominant fungal stages we observed were extra- and intraradical hyphae. Jentschel and others (2007) have recently shown that an auxin inducible promoter-GUS reporter construct in tobacco gave an indication of higher auxin signals in AM roots compared to controls, but there was no clear correlation with AM structures such as hyphae and arbuscules. However, at the moment additional routes for the increased levels of IBA in AM-inoculated roots cannot be ruled out.

MtIAR33 appears to be involved in auxin release also during AM formation, together with MtIAR34 (Figure 5). However, in AM formation MtIAR34 is not as strongly upregulated as during nodulation and MtIAR33 is comparable in expression to –34. Unlike the rhizobial induction, the expression pattern during AM formation is more likely to reflect overlapping enzymatic function between several hydrolytic enzymes. MtIAR33 and –34 both have strong activity against IAA-Asp, whereas MtIAR34 also has activity against the ester conjugate IAA-glucose. It is important to point out that even though MtIAR33 is not relatively induced in the whole plant or tissues, its functional importance is signified by its upregulation during symbiotic interactions.

Our results indicate an intricate, overlapping control system that regulates free and conjugated auxins in *Medicago*. These control systems appear to manage housekeeping functions such as stem and root development, but they also elaborately regulate the early stages of AM formation and nodulation. We will continue to examine the regulation of the hydrolases involved in these control processes, including the occurrence of auxin conjugates in *Medicago*, and try to better understand what happens to these complicated schemes when the hydrolytic regulatory systems are impaired or mutated.

Acknowledgments This work was supported by a Sokol grant for undergraduate research. The authors thank Dr. Melanie Jean Barnett from Stanford University for the gift of the *Sinorhizobium meliloti* 1021 strain. The technical assistance of Silvia Heinze is gratefully acknowledged. The authors also thank Lisa Campanella for her generous editorial help.

References

Altschul SF, Gish W, Miller W, Myers EW, Lipman DJ (1990) Basic Local Alignment Search Tool. J Mol Biol. 215(3):403–410

Baldi BG, Maher BR, Cohen JD (1989) Hydrolysis of indole-3-acetic acid esters exposed to mild alkaline conditions. Plant Physiol 91:9–12

Bandurski RS, Cohen JD, Slovin JP, Reinecke DM (1995) Auxin biosynthesis and metabolism. In: Davies PJ (ed), Plant Hormones: Physiology, Biochemistry and Molecular Biology, 2nd edn. Boston: Kluwer Academic Publishers, pp 39–65

Barker SJ, Tagu D (2000) The roles of auxins and cytokinins in mycorrhizal symbiosis. J Plant Growth Regul 19:144–154

Bartel B, Fink G (1995) ILR1, an amidohydrolase that releases active indole-3-acetic acid from conjugates. Science 268:1745–1748

Caetano-Anollés G, Gresshoff PM (1991) Plant genetic control of nodulation. Annu Rev Microbiol 45:345–382

Campanella JJ, Ludwig-Müller J, Town CD (1996) Isolation and characterization of mutants of *Arabidopsis thaliana* with increased resistance to growth inhibition by indoleacetic acid-amino acid conjugates. Plant Physiol 112:735–745

Campanella JJ, Bakllamaja V, Restieri T, Vomacka M, Herron J, Patterson M, Shahtaheri S (2003a) Isolation of an ILR1 auxin conjugate hydrolase homologue from *Arabidopsis suecica*. Plant Growth Regul 39:175–181

Campanella JJ, Larko D, Smalley J (2003b) A molecular phylogenomic analysis of the ILR1-like family of IAA amidohydrolase genes. Comp Funct Genom 4:584–600

Campanella JJ, Ludwig-Müller J, Bakllamaja V, Sharma V, Cartier A (2003c) ILR1 and sILR1 IAA amidohydrolase homologues differ in expression pattern and substrate specificity. Plant Growth Regul 41:215–223

Campanella JJ, Olajide A, Magnus V, Ludwig-Müller J (2004) A novel auxin conjugate from wheat with substrate specificity for longer side-chain auxin amide conjugates. Plant Physiol 135:2230–2240

Ceroni A, Frasconi P, Passerini A, Vullo A (2003) Predicting the disulfide bonding state of cysteines with combinations of kernel machines. J VLSI Signal Processing 35:287–295

Chou J-C, Mulbry WW, Cohen JD (1998) The gene for indole-3-acetyl-L-aspartic acid hydrolase from *Enterobacter agglomerans*: molecular cloning, nucleotide sequence, and expression in *Escherichia coli*. Mol Gen Genet 259:172–178

Chou J-C, Welch WH, Cohen JD (2004) His-404 and His-405 are essential for enzyme catalytic activities of a bacterial indole-3-acetyl-L-aspartic acid hydrolase. Plant Cell Physiol 45:1335–1341

Cohen JD (1984) Convenient apparatus for the generation of small amounts of diazomethane. J Chromatogr 303:193–196

Cohen JD, Bandurski RS (1982) The chemistry and physiology of the bound auxins. Annu Rev Plant Physiol 33:403–430

Cohen JD, Baldi BG, Slovin JP (1986) $^{13}C_6$-[benzene ring] - indole-3-acetic acid. Plant Physiol 80:14–19

Cook D, van der Bosch K, de Bruijin F, Huguet T (1997) Model legumes get the nod. Plant Cell 9:275–281

Davies RT, Goetz DH, Lasswell J, Anderson MN, Bartel B (1999) IAR3 encodes an auxin conjugate hydrolase from *Arabidopsis*. Plant Cell 11:365–376

de Billy F, Grosjean C, May S, Bennett M, Cullimore JV (2001) Expression studies on AUX1-like genes in *Medicago truncatula* suggest that auxin is required at two steps in early nodule development. Mol Plant Microbe Interact 14:267–277

Ehrhardt DW, Atkinson EM, Long SR (1992) Depolarization of alfalfa root hair membrane potential by *Rhizobium meliloti* Nod factors. Science 256:998–1000

Felsenstein J (1985) Confidence limits on phylogenies: An approach using the bootstrap. Evolution 39:783–791

Fitze D, Wiepning A, Kaldorf M, Ludwig-Müller J (2005) Auxins in the development of an arbuscular mycorrhizal symbiosis in maize. J Plant Physiol 162: 1210–1219

Hirsch AM, La Rue TA (1997) Is the legume nodule a modified root or stem or an organ sui generis? Crit Rev Plant Sci 16:361–392

Hirsch AM, Bhuvaneswari TV, Torrey JG, Bisseling T (1989) Early nodulin genes are induced in alfalfa root outgrowths elicited by auxin transport inhibitors. Proc Natl Acad Sci USA 86:1244–1248

Hirsch AM, Fang Y, Asad S, Kapulnik Y (1997) The role of phytohormones in plant-microbe symbioses. Plant Soil 194:171–184

Huo X, Schnabel E, Hughes K, Frugoli J (2006) RNAi phenotypes and the localization of a protein::GUS fusion imply a role for *Medicago truncatula PIN* genes in nodulation. J Plant Growth Regul 25:156–165

James LC, Tawfik DS (2001) Catalytic and binding poly-reactivities shared by two unrelated proteins: The potential role of promiscuity in enzyme evolution. Protein Sci 10:2600–2607

Jensen RA (1976) Enzyme recruitment in evolution of new function. Annu Rev Microbiol 30:409–425

Jentschel K, Thiel D, Rehn F, Ludwig-Müller J (2007) Arbuscular mycorrhiza enhances auxin levels and alters auxin biosynthesis in *Tropaeolum majus* during early stages of colonization. Physiol Plant 129:320–333

Kaldorf M, Ludwig-Müller J (2000) AM fungi might affect the root morphology of maize by increasing indole-3-butyric acid biosynthesis. Physiol Plant 109:58–67

LeClere S, Tellez R, Rampey RA, Matsuda SPT, Bartel B (2002) Characterization of a family of IAA-amino acid conjugate hydrolases from *Arabidopsis*. J Biol Chem 277:20446–20452

Lu Z, Szafron D, Greiner R, Lu P, Wishart DS, Poulin B, Anvik J, Macdonell C, Eisner R (2004) Predicting subcellular localization of proteins using machine-learned classifiers. Bioinformatics 20(4):547–556

Ludwig-Müller J (2000) Hormonal balance in plants during colonization by mycorrhizal fungi. In: Douds DD, Kapulnik Y (eds), Arbuscular Mycorrhizas: molecular biology and physiology. Dordrecht: Kluwer Academic Publishers, pp 263–285

Ludwig-Müller J, Cohen JD (2002) Identification and quantification of three active auxins in different tissues of *Tropaeolum majus*. Physiol Plant 115:320–329

Ludwig-Müller J, Güther M (2007) Auxins as signals in arbuscular mycorrhiza formation. Plant Signaling Behav 2: 194–196

Ludwig-Müller J, Epstein E, Hilgenberg W (1996) Auxin-conjugate hydrolysis in Chinese cabbage: Characterization of an amidohydrolase and its role during infection with clubroot disease. Physiol Plant 97:627–634

Ludwig-Müller J, Kaldorf M, Sutter EG, Epstein E (1997) Indole-3-butyric acid (IBA) is enhanced in young maize (*Zea mays* L.) roots colonized with the arbuscular mycorrhizal fungus *Glomus intraradices*. Plant Sci 125:153–162

Mathesius U, Schlamann HRM, Spaink HP, Sautter C, Rolfe BG, Djordjevic MA (1998) Auxin transport inhibition precedes root nodule formation in white clover roots and is regulated by flavonoids and derivatives of chitin oligosaccharides. Plant J 14:23–34

Meixner C, Ludwig-Müller J, Miersch O, Gresshoff P, Staehelin C, Vierheilig H (2005) Lack of mycorrhizal autoregulation and phytohormonal changes in the supernodulating soybean mutant nts1007. Planta 222:709–715

Mulder L, Hogg B, Bersoult A, Cullimore JV (2005) Integration of signalling pathways in the establishment of the legume-rhizobia symbiosis. Physiol Plant 123:207–218

Pacios-Bras C, Schlaman HRM, Boot K, Admiraal P, Langerak JM, Stougaard J, Spaink HP (2003) Auxin distribution in *Lotus japonicus* during root nodule development. Plant Mol Biol 52:1169–1180

Page RD (1996) TREEVIEW: An application to display phylogenetic trees on personal computers. Comput Appl Biosci 12:357–358

Rampey RA, LeClere S , Kowalczyk M, Ljung K, Sandberg G, Bartel B (2004) A family of auxin-conjugate hydrolases that contributes to free indole-3-acetic acid levels during *Arabidopsis* germination. Plant Physiol 135:979–988

Roodveldt C, Tawfik DS (2005) Shared promiscuous activities and evolutionary features in various members of the amidohydrolase superfamily. Biochemistry 44:12728–12736

Roudier F, Fedorova E, Lebris M, Lecomte P, Gyorgyey J, Vaubert D, Horvath G, Abad P, Kondorosi A, Kondorosi E (2003) The *Medicago* species A2-type cyclin is auxin regulated and involved in meristem formation but dispensable for endoreduplication-associated developmental programs. Plant Physiol 131:1091–1103

Saitou N, Nei M (1987) The neighbor-joining method: A new method for reconstructing phylogenetic trees. Mol Biol Evol 4:406–425

Sambrook J, Maniatis T, Fritsch EF (1989) Molecular Cloning: A Laboratory Manual, 2nd edn, vol 1. Cold Spring Harbor, NY: Cold Spring Harbor Laboratory Press, pp 31–112

Schmitz O, Danneberg G, Hundeshagen B, Klingner A, Bothe H (1991) Quantification of vesicular-arbuscular mycorrhiza by biochemical parameters. J Plant Physiol 139:106–111

Schuller A, Ludwig-Müller J (2006) A family of auxin conjugate hydrolases from *Brassica rapa*: Characterization and expression during clubroot disease. New Phytol 171:145–158

Stors G, Opdyke JA, Zhang A (2004) Controlling mRNA stability and translation with small noncoding RNAs. Curr Opin Microbiol 7:140–144

Sutter EG, Cohen JD (1992) Measurement of indolebutyric acid in plant tissues by isotope dilution gas chromatography-mass spectrometry analysis. Plant Physiol 99:1719–1722

Thompson JD, Gibson TJ, Plewniak F (1997) The Clustal X Windows interface: flexible strategies for multiple sequence alignment aided by quality analysis tools. Nucleic Acids Res 24:4872–4882

Vierheilig H (2004) Regulatory mechanisms during the plant-arbuscular mycorrhizal fungus interaction. Can J Bot 82:1166–1176

Vullo A, Frasconi P (2004) Disulfide connectivity prediction using recursive neural networks and evolutionary information. Bioinformatics 20:653–659

Walz A, Park S, Slovin JP, Ludwig-Müller J, Momonoki YS, Cohen JD (2002) A gene encoding a protein modified by the phytohormone indoleacetic acid. Proc Natl Acad Sci U S A 99:1718–1723

Wasson AP, Pellerone FI, Mathesius U (2006) Silencing the flavonoid pathway in *Medicago truncatula* inhibits root nodule formation and prevents auxin transport regulation by rhizobia. Plant Cell 18:1617–1629

Wells G, Huston C (1995) High-resolution selected ion monitoring in a quadrupole ion trap mass spectrometer. Anal Chem 67:3650–3655